New Genicular Joint Angle Criteria for Flexor Muscle (*Musculus Semimembranosus*) during the Terrestrial Mammals Walking

Fumihiro Mizuno [Corresp., 1] , **Naoki Kohno** [1, 2]

[1] Life and Environmental Science, University of Tsukuba, Tsukuba, Ibaraki, Japan

[2] National Museum of Nature and Science, Tsukuba, Ibaraki, Japan

Corresponding Author: Fumihiro Mizuno
Email address: f.mizuno.86.09@gmail.com

Background. The genicular or knee joint angles of terrestrial mammals remain constant during the stance phase of walking; however, the angles differ among taxa. The knee joint angle is known to correlate with taxa and body mass among extant mammals, yet several extinct mammals, such as desmostylians, do not have closely related descendants. Furthermore, fossils lose their soft tissues by the time they are unearthed, making body mass estimates difficult. These factors cause significant problems when reconstructing the proper postures of extinct mammals. Terrestrial mammals use potential and kinetic energy for locomotion; particularly, an inverted pendulum mechanism is used for walking. This mechanism requires maintaining the rod length constant, therefore, terrestrial mammals maintain their joint angle in a small range. A muscle reaction referred to as co-contraction is known to increase joint stiffness; both the agonist and antagonist muscles work simultaneously on the same joint at the same time. The *musculus semimembranosus* flexes the knee joint and acts as an antagonist to muscles that extend it.

Methods. Twenty-one species of terrestrial mammals were examined to identify the elements that constitute the angle between the *m. semimembranosus* and the tibia based on the period between the hindlimb touching down and taking off from the ground. Measurements were captured from videos in high-speed mode (420 fps), selecting 13 pictures from the first 75 % of each video while the animals were walking. The angles between the main force line of the *m. semimembranosus* and the tibia, which were defined as θ_{sm-t}, were measured.

Results. The maximum and minimum angles between the *m. semimembranosus* and the tibia (θ_{sm-t}) of the stance instance (SI) were successfully determined for more than 80% of the target animals (17 out of 21 species) during SI-1 to SI-13 within ± 10 ° from the mean. The difference between each successive SI was small and, therefore, the θ_{sm-t} transition was smooth. According to the results of the total stance differences among the target animals, θ_{sm-t} was relatively constant during a stance and, therefore, average θ_{sm-t} (θ_{ave}) can represent each animal. Only Carnivora had a significant difference in the correlation between body mass and θ_{ave}. In addition, there were significant differences in θ_{ave} between plantigrade and unguligrade locomotion.

Conclusion. Our measurements show that θ_{ave} was 100 ± 10 ° regardless taxon, body mass, and locomotor mode. Thus, only three points on skeletons need to be measured to determine θ_{ave}. This offers a new approximation approach for understanding hindlimb posture that could be applied to the study of the hindlimbs of extinct mammals with no closely related extant descendants.

1 # New Genicular Joint Angle Criteria for Flexor Muscle

2 # (*Musculus Semimembranosus*) during the Terrestrial

3 # Mammals Walking

6 Fumihiro Mizuno[1] and Naoki Khono[1,2]

8 [1]Graduate school of Life and Environmental Science, University of Tsukuba, Ibaraki, Japan,

9 [2]National Museum of Nature and Science, Ibaraki, Japan

11 Correspondence: Fumihiro Mizuno

12 1-1-1 Tennodai,Tsukuba, Ibaraki, 305-8572, Japan

13 Email: fmizuno86@geol.tsukuba.ac.jp

15   **Abstract**

16   **Background.** The genicular or knee joint angles of terrestrial mammals remain constant during

17   the stance phase of walking; however, the angles differ among taxa. The knee joint angle is

18   known to correlate with taxa and body mass among extant mammals, yet several extinct

19   mammals, such as desmostylians, do not have closely related descendants. Furthermore, fossils

20   lose their soft tissues by the time they are unearthed, making body mass estimates difficult.

21   These factors cause significant problems when reconstructing the proper postures of extinct

22   mammals. Terrestrial mammals use potential and kinetic energy for locomotion; particularly, an

23   inverted pendulum mechanism is used for walking. This mechanism requires maintaining the rod

24   length constant, therefore, terrestrial mammals maintain their joint angle in a small range. A

25   muscle reaction referred to as co-contraction is known to increase joint stiffness; both the agonist

26   and antagonist muscles work simultaneously on the same joint at the same time. The *musculus*

27   *semimembranosus* flexes the knee joint and acts as an antagonist to muscles that extend it.

28   **Methods.** Twenty-one species of terrestrial mammals were examined to identify the elements

29   that constitute the angle between the m. semimembranosus and the tibia based on the period

30   between the hindlimb touching down and taking off from the ground. Measurements were

31   captured from videos in high-speed mode (420 fps), selecting 13 pictures from the first 75 % of

32   each video while the animals were walking. The angles between the main force line of the *m.*

33   *semimembranosus* and the tibia, which were defined as θ_{sm-t}, were measured.

34   **Results.** The maximum and minimum angles between the *m. semimembranosus* and the tibia

35   (θ_{sm-t}) of the stance instance (SI) were successfully determined for more than 80% of the target

36   animals (17 out of 21 species) during SI-1 to SI-13 within $\pm 10\ °$ from the mean. The difference

37   between each successive SI was small and, therefore, the θ_{sm-t} transition was smooth. According

38   to the results of the total stance differences among the target animals, θ_{sm-t} was   relatively

39   constant during a stance and, therefore, average θ_{sm-t} (θ_{ave}) can represent each animal. Only

40   Carnivora had a significant difference in the correlation between body mass and θ_{ave}. In addition,

41   there were significant differences in θ_{ave} between plantigrade and unguligrade locomotion.

42   **Conclusion.** Our measurements show that θ_{ave} was $100 \pm 10\ °$ regardless taxon, body mass, and

43   locomotor mode. Thus, only three points on skeletons need to be measured to determine θ_{ave}.

44   This offers a new approximation approach for understanding hindlimb posture that could be

45   applied to the study of the hindlimbs of extinct mammals with no closely related extant

46   descendants.

47

Introduction

Hindlimbs act as propulsive devices for terrestrial locomotion (Demes et al., 1994). Common terrestrial behaviors require limbs to support body mass against gravity, which means that terrestrial mammals must resist collapsing joints against gravity, requiring the maintenance of extending joints. Although limbs have the same role in that supporting body mass, joint angles differ between species (Biewener, 1983, 2005; Inuzuka, 1996; Dutto et al., 2006; Polly, 2007; Fujiwara, 2009; Dick & Clemente, 2017). For example, the angles at the knee joint in Asian elephants is approximately 160 ° (Ren et al., 2008), compared to 137 ° in chacma baboons (Patel et al., 2013), 115 ° in domestic cats, 124 ° in lions (Day & Jayne, 2007). Thus, the limb joint angle is unique to each species; however, the joints have a wider rotatable range than the angle maintained during standing or walking. This causes problems when reconstructing skeletal specimens into an accurate posture when they were alive. In particular, extinct taxa present a significant challenge when reconstructing postures because the angle when they were alive cannot be observed. For example, desmostylian mammals, which do not have closely related living descendants, have been reconstructed in several different postures even though almost complete skeletons of the same species have been unearthed (Domning, 2002; Inuzuka, Sawamura & Watabe, 2006; Fujiwra, 2009). Furthermore, earlier diverging cetaceans, such as pakicetids and ambulocetids, had functional hindlimbs, and extant cetaceans had completely lost their hindlimbs (Thewissen, Madar, & Hussain, 1998; Gingerich, 2001; Thewissen et al., 2001; Madar, 2007; Gingerich et al., 2009; Gingerich et al., 2017). In such cases, there are no extant mammals that can be used as references for skeletal reconstruction. Therefore, knowledge of hindlimb postures in terrestrial mammals is important to understand the transition of locomotive ability through mammalian evolution, including the adaptation from land to sea.

Several studies have explored the relationship between limb posture and variables such as taxa, body mass, and skeletal morphology in extant mammals (Biewener, 1983, 1989, 1990, 2005; Day & Jayne, 2007; Fujiwara, 2009; Fujiwara & Hutchinson, 2012: Dick & Clemente, 2017). These studies indicate that the larger the size of the mammal species the more upright limb posture the species has. However, there are several exceptions to the relationship between limb posture and body mass (Fujiwara, 2009). Furthermore, there is a significant problem with estimating the body mass of extinct mammals because fossils have already lost soft tissues by the time they are unearthed. To resolve these problems, it is important to identify joint angle criteria that are unaffected by other factors as possible.

Quadrupedal mammals use potential and kinetic energy to accelerate their center of mass during running and walking (Cavagna, Heglund & Taylor, 1977; Alexander & Jayes, 1978; Hildebrand,

84   1984; Hildebrand & Hurley, 1985; Alexander, 1991; Griffin, Main & Farley, 2004), employing
85   an inverted pendulum movement to walk. This movement allows the quadrupedal mammals to
86   generate the necessary energy to lift and accelerate the center of mass and maintain a constant
87   stride length (Cavagna, Heglund & Taylor, 1977; Griffin, Main & Farley, 2004). The inverted
88   pendulum requires that the distance between the ground and the center of mass is constant;
89   therefore, the limb joints are maintained within limited range while walking (Manter, 1938;
90   Gray, 1944; Goslow, Reinking & Stuart, 1973; Goslow et al., 1981; Alexander & Jayes, 1983;
91   Inuzuka, 1996; Fischer et al., 2002; McGowan, Baudinette & Biewener, 2005). When a joint
92   angle is locked against the force of gravity, not only the agonist muscle but also the antagonist
93   muscle work together. This action increases joint stiffness in humans (Olmstead et al., 1986;
94   Louie & Mote, 1987; Nielsen et al., 1994; Riemann & Lephart, 2002; Knarr, Zeni & Higginson,
95   2012). Some electromyographic studies of quadrupedal mammals have shown that both agonist
96   and antagonist muscles act simultaneously during the stance phase—the period in which the foot
97   under consideration is in contact with the floor— when the limb supports the body mass
98   (Engberg & Lundberg, 1969; Tokuriki, 1973; Deban, Schilling & Carrier, 2012; Araújo et al.,
99   2016). The knee joint maintains an angle owing to extension against gravity, and the *musculus*
100   *semimembranosus* acts as the knee joint flexor muscle, which is the antagonist muscle of the *m.*
101   *quadriceps femoris* when the joint extends.
102
103   The *m. semimembranosus* attaches to the ischial tuberosity and interior proximal end of the tibia
104   (Fig. 1) (Böhmer. Et al., 2020). These attachment positions do not move, and the involved parts
105   of the skeleton do not change their shape greatly among taxa. Thus, the positional relationship
106   between the muscle and these parts of the skeleton also shows the relationship among skeleton
107   elements. In addition, the angles of the pelvic girdle differ among different body masses (Polly,
108   2007). Therefore, the angle between the line of action of the *m. semimembranosus* and the tibia
109   has a smaller difference than the angle between the femur and tibia among different body
110   masses. Here, we aimed to (1) reveal the joint angle of terrestrial mammals between the *m.*
111   *semimembranosus* and tibia during walking, (2) explore the relationships between this angle and
112   taxa, body mass, and locomotor mode, and (3) evaluate whether this angle might be suitable as
113   one of the criteria for the reconstruction of hindlimb postures.
114

115   **Materials & Methods**
116   The angles between *m. semimembranosus* and the tibia *in vivo* were collected from 21 extant
117   species from 21 genera and 14 families within seven orders (Table 1). These species were
118   selected to cover the superorder and order of mammals (Afrotheria, Proboscidea;
119   Euarchontoglires, Primates, Rodentia; Laurasiatheria, Artiodactyla, Carnivora, Perissodactyla;

120 and Marsupialia, Diprotodontia), a wide range of body masses (i.e., from 0.7 kg for *Suricata*
121 *suricatta* to 4,060 kg for *Elephas maximus*), and three locomotor modes (plantigrade, digitigrade,
122 and unguligrade) (Table 1). All the target animals were kept in zoos at Higashi Park Zoological
123 Gardens (Okazaki, Japan), Higashiyama Zoo and Botanical Garden (Aichi, Japan), Hitachi
124 Kaminé Zoo (Ibaraki, Japan), Toyohashi Zoo and Botanical Park (Aichi, Japan), and Ueno
125 Zoological Gardens (Tokyo, Japan), and all observations of living individuals were conducted
126 after gaining official permissions. No significant pathologies or malformations were detected in
127 any of the studied specimens.
128
129 All target animals were subjected to video recording using a digital movie camera (EX-FH20,
130 Casio, Japan) in high-speed mode (420 fps). The camera was mounted on a tripod along the
131 visitor viewing route. Therefore, the distance from each target depended on the exhibition/cage
132 arrangement. All videos were taken from the lateral side and at nearly the same level as the target
133 animal when they walked vertically and completely (without stopping, turning, or changing
134 speed) with the camera on flat ground. We waited until each target walked across the camera
135 voluntarily, without any coaxing, meaning it took several weeks or months to obtain the required
136 video footage.
137 We selected three videos of each target species that walked with one complete cycle (touching
138 down to the next touching down), straight, and vertical to the camera. Each video was then
139 converted into still images of every frame during the period between touching down and taking
140 off using the GOM Player (GOM & Company, South Korea). This period did not depend on time
141 but on the target's behavior. The convert images from the last 25% of each batch (for each
142 measurement period) were discarded because "the muscles that are anatomically positioned to
143 produce limb retraction – the *gluteus superficialis* and *medius*, *semimembranosus* and cranial
144 *biceps femoris* – were active in the second half of swing and approximately the first 50–75% of
145 stance" (Deban, Schilling & Carrier, 2012). Subsequently, the first 75% of the stance phase of
146 each step for every specimen was divided into 12 equal time periods (particularly for each step)
147 to obtain 13 images, including the first and last frames. (Fig. 2A). The following lines were then
148 drawn on each of the 13 pictures using Inkscape (Inkscape project) and the angle between them
149 was measured: a line between the ankle joint and the proximal end of the tibia parallel to the
150 Achilles tendon, and a line between the ischial tuberosity and the proximal end of the tibia (Fig.
151 2B).
152
153 We defined each image of the 13 pictures as a "stance instance" (SI) and numbered them as SI-1
154 to SI-13. The combination of these 13 images defined a series of a single stance. We measured
155 the joint angle between the lines in each of the 13 images, in each stance, and three stances for

156 each target species in this way. The average angle of each SI was defined as θ_{sm-t}. The body mass

157 of each species was obtained from the literature (Table 1) or zoo records. We compared the

158 transition of θ_{sm-t} in a stance among species and locomotor modes (unguligrade, digitigrade, and

159 plantigrade), and the average θ_{sm-t} values (i.e., θ_{ave}) against body mass. Statistical analyses were

160 performed using R software package (The R Project for Statistical Computing, Vienna, Austria).

161 We calculated the standard deviation (SD) to compare the variance of θ_{sm-t} among taxa, SIs, and

162 locomotor modes. We also calculated correlation coefficient (r) to examine relationships

163 between body mass, and θ_{ave} and performed analysis of variance (ANOVA) to clarify the

164 relationships of θ_{ave} with body mass, taxa and locomotor modes. For the comparison between θ_{ave}

165 and body mass, the studied species were divided into the following groups: < 1, < 10, < 100, <

166 1,000, and ≥ 1,000 kg. The orders and locomotor modes used for the analyses were the same as

167 in the tables. In addition, data that had only one taxon were eliminated, specifically *Elephas*,

168 *Dolichotis*, and *Macropus* in the analysis between taxa; *Macropus* in the locomotor mode

169 comparison; and *Suricata* in the body mass comparison (Tables 1).

170

171 **Results**

172 Six taxa, i.e., *Elephas* (Proboscidea)*, Cervus* and *Rangifer* (Artiodactyla), *Tapirus*

173 (Perissodactyla), and *Felis* and *Panthera* (Carnivora) had differences of less than 10 ° between

174 the maximum and minimum angles during a stance, which means that θ_{sm-t} changed within ± 5 °

175 from the middle. Of the species, *Cervus* had the smallest difference during a stance, 5.80 ° (±2.9

176 ° from the middle-value) . Twelve taxa, i.e., *Chlorocebus* and *Macaca* (Primates), *Dolichotis*

177 (Rodentia), *Ammotragus*, *Capra*, and *Giraffa* (Artiodactyla), *Canis*, *Chrysocyon*, *Suricata* and

178 *Helarctos* (Carnivora), and *Equus* and *Diceros* (Perissodactyla), had differences between the

179 maximum and the minimum angles during a stance of between 10 and 20 °, which means that

180 θ_{sm-t} changed within ± 10 ° from the middle-value. Two taxa, i.e., *Ursus* (Carnivora), and

181 *Ceropithecus* (Primates) had differences between the maximum angle and minimum angle

182 during a stance of less than 30 °, which means that θ_{sm-t} changed within ± 15 ° from the middle-

183 value. While *Macropus* (Diprotodontia) had the largest difference between the maximum and

184 minimum angles during a stance, (31.8 °),   with θ_{sm-t} changing within ± 16 ° from the middle-

185 value, *Panthera* had the lowest SD (1.73 ° while *Macropus* had the largest one (11.5 °; Fig. 3

186 and Table 2).

187 Based on the differences between each SI among all target species, SI-1 had the smallest

188 difference at 41.5 °, and SI-13 had the largest difference at 54.8 °. However, the smallest SD was

189 observed for SI-4 (10.03 °), while the largest statistically significant SD was for SI-13, (12.81 °;

190 Table 2). This is because the low θ_{sm-t} value for *Suricata* is considered as an outlier in SI-13(Fig.

191 4). Taxonomically, Carnivora had the greatest difference between the largest and smallest angles

192 for the same SI, being 54.8 ° in SI-13; this order had relatively high differences compared to the
193 other taxa at every SI, exceeding 30 ° in each case (Table 2). The smallest difference was
194 observed in Primates, being 2.9 ° in SI-7; this order had relatively low differences compared to
195 the other taxa in nine out of the 13 SIs (Table 2). Based on locomotion, digitigrade species have
196 higher difference in SI-11 (52.7 °; Table 3), while digitigrade had relatively high differences in
197 all SIs, exceeding 38 ° in every case. The differences for unguligrade and plantigrade fell
198 between 11.8 ° and 23.3 ° (Table 3). Except for *Elephas* and *Macropus*, all of the examined
199 species had positive values when θ_{sm-t} of SI-2 was subtracted from SI-1, while when subtracting
200 the values SI-2 from SI-3 values were positive for all species except *Cervus* and *Rangifer*. This
201 indicates that these species, *Cervus*, *Rangifer*, *Elephas* and *Macropus*, started their stance phase
202 by flexing the knee joint. The number of species with negative values increase in the subsequent
203 steps, but the values soon became positive. The subtracted values of successive SIs were
204 repeatedly positive and negative with in short span up to SI-9 and most species presented
205 negative values after SI-10, showing extension of the knee joint when finishing the stance phase.
206 The difference between successive SIs did not exceed 10 ° in any species, therefore, θ_{sm-t}
207 smoothly transited and changed in small amounts during a stance phase (Table 4).
208
209 According to the results of the θ_{sm-t} transition analysis, every studied species had relatively small
210 differences between maximum and minimum θ_{sm-t} values during the stance phase (Figs. 3 and 4,
211 Table 2). This showed that the total stance differences among the target animals were small;
212 thus, θ_{ave} values were representative of each species. Accordingly, we analyzed the relationships
213 between θ_{ave} and body mass. The resulting correlation coefficient (*r*) for all target animals was
214 0.30 with a p-value of 0.19 and 19 degrees of freedom (d.f.; Table 5). The correlation between
215 the body mass and θ_{ave} of each taxon was also calculated, which was significant only for
216 Carnivora (*r* = 0.81, *p* = 0.028, d.f. = 5). The correlation between body mass and θ_{ave} for each
217 locomotor mode was only significant for digitigrade (*r* = 0.88, *p* = 0.01, d.f. = 5; Table 5). Thus,
218 there was no statistically significant correlation between θ_{ave} and body mass except for Carnivora
219 and digitigrade. Furthermore, the θ_{ave} of all species was 99.7 °, with the smallest being that of
220 *Suricata* (73.0 °), with the largest that of *Elephas* (120.7 °). Therefore, more than 80 % of the
221 targets (17/21) had an angle between 90 ° and 110 ° (Table 2) including all Artiodactyla,
222 Perissodactyla, and five of the seven Carnivora assessed in our study.
223 ANOVAs of θ_{ave} values were used to compare taxa, locomotor mode, and body mass. Only
224 locomotor mode was statistically significant (*p* = 0.049; Table 6A). Furthermore, the multiple
225 comparisons among locomotor modes showed a significant difference between unguligrade and
226 plantigrade species (*p* = 0.04; Table 6B).
227

Discussion

Quadrupedal animals use their limbs for inverted pendulum-like movements (Cavagna, Heglund & Taylor, 1977; Griffin, Main & Farley, 2004). Physically, the swing velocity depends on the rod length; in terrestrial mammals, the swing speed affects the walking velocity. In this regard, limbs are the only structure that control the distance between the ground and body trunk; therefore, the rod length depends on the joint angles. The knee joint receives forces to flex from several influencing factors, such as the collision at touchdown, gravity, and a rising the center of mass. This means that the extensor muscles react immediately against flexion. In addition, quadrupedal mammals recovered up to 70% of their mechanical energy to lift and accelerate their center of mass *via* an inverted pendulum mechanism (Griffin, et al., 2004). Therefore, the joint angle should also be maintained constant to keep the length of the pendulum arm. Co-contraction also occurs to increase joint stiffness (Hogan, 1984), i.e., flexor and extensor muscles are stimulated at the same time. Previous studies focused on the position of the femur while, in our study, we center the attention on the location of the ischial tuberosity of the pelvis. As the pelvis does not rotate drastically during walking, this logic also applies to θ_{sm-t}. Each examined stance showed different results than our expectation, that extension and flexion periods were not completely separated as in the case of extension in the first half of a stance and flexion in the later half. The difference between θ_{sm-t} in successive SIs showed that joint flexion and extension were repeated over a short timespan (Table 4). The alternating increase and decrease in θ_{sm-t} between each SI allow quadrupedal mammals to maintain joint angles. In other words, the role of co-contraction during walking is not to fix the joint angles but to maintain the joint angles within a certain range, involving small increases and decreases in θ_{sm-t} across the broad range of studied taxa (Table 4). Therefore, the θ_{sm-t} angle transitions during one stance were small among the target species. Furthermore, the angle transition waveforms resembled among studied species (Fig. 4). *Macropus* had a unique waveform because they support their body with a tail and move both hindlimbs together (O'Connor et al., 2014). This walking pattern was found only in *Macropus*. Although there are different waveforms, we found that 18 out of 21 target species had only slight differences in θ_{sm-t} change (less than $\pm 10°$ from the middle value) even though the largest difference was $\pm 15.86°$ (Fig. 3 and 4 and Table 2).

The θ_{ave} values of most of the studied species (>80 %) were $100 \pm 10°$ (i.e., excluded species are *Elephas*, *Dolichotis*, *Helarctos* and *Suricata*; Table 2 and Fig 5) including those of all three locomotor modes (i.e., unguligrade, digitigrade, and plantigrade), and five out of seven orders (i.e., Primates, Artiodactyla, Carnivora, Perissodactyla, and Marsupialia), with slight differences between unguligrade and plantigrade ($p = 0.04$; Table 6B, Fig. 6). Species within this range also had a wide range of the body masses, from 4.8 kg (*Felis*) to 1100 kg (*Diceros*; Table 1 and 3).

264   The effective mechanical advantage (EMA) is one means of estimating mammalian limb posture;

265   the larger EMA, the more upright the posture, with the largest species typically having greater

266   EMA (Biewener, 1898,1990, 2005; Dick & Clemente, 2017). Even when for the new

267   measurement proposed in our work a slight correlation can be observed between the knee angle

268   and body mass (Fig. 5), this correlation is not significant ($r = 0.3$ and $p = 0.19$, d.f. = 19), when

269   considering all studied species. Also, our findings show that θ_{ave} is much less variable than

270   EMA. Such a difference between studies is due to the differences in angle-measurement

271   positions. The ischial tuberosity, to which the *m. semimembranosus* is attached, is located near

272   the posterior end of the pelvis. The horizontal or vertical orientation of the pelvis is related to

273   body mass, with a larger body mass having a more upright orientation (Polly, 2007). Therefore, a

274   larger body mass has a larger difference between the angle of the femur-tibia (the traditional

275   knee joint angle, as previously standardized) than the *m. semimembranosus*-tibia (θ_{sm-t} and θ_{ave},

276   as proposed in our study). In other words, θ_{em-t} and θ_{ave} have the advantage of reflecting the small

277   differences between these angles in large-body-mass species and small body mass species.

278   Furthermore, the EMA does not increase linearly above species weighing 300 kg (Biewener,

279   1990, 2005; Dick & Clemente, 2017), and felids have a crouched posture even with a larger body

280   mass (Day & Jayne, 2007; Dick & Clemente, 2017). In contrast, θ_{ave} shows constant values (100

281    $\pm 10\ °$) among all locomotor modes and a wide body mass range (4.5–1100 kg; Table 1 and 3).

282

283   In addition, we measured θ_{sm-t} based on three points on the skeleton the ischial tuberosity

284   interior-proximal end of the tibia, and distal end of the tibia (Fig. 1). This indicates that the

285   position of the ischial tuberosity and tibia can be fixed with $100 \pm 10\ °$ on extant terrestrial

286   quadrupedal mammals, including those with no closely related extant descendants. If a femur

287   exists or its shape can be estimated, the limb posture can be reconstructed with higher accuracy

288   using our approach because both the caput femoris and the distal end of the femur can be placed

289   in the determined positions, which are the acetabulum and the proximal end of the tibia,

290   respectively. For example, Desmostylia has been previously reconstructed in several different

291   postures even whole-body skeletons exist (Shikama, 1966; Inuzuka, 1988; Domning, 2002;

292   Inuzuka, Sawamura & Warabe, 2006). Because this extinct mammal has no closely related

293   descendants and has an extremely unusual tibia, the distal half of the tibia is strongly medially

294   twisted by approximately about $40\ °$ (Shikama, 1966; Inuzuka, 1988), no extant mammals have

295   tibias resembling to those of Desmostylia. The θ_{ave} value, which is $100 \pm 10\ °$, is not strongly

296   affected by taxonomy, body mass, and locomotor mode, and therefore, this degree can be applied

297   to Desmostylia.

298

299   **Conclusion**

300   Stimulation of the agonist and antagonist muscles, known as co-contraction, increases joint

301   stiffness. In the case of the knee joint angle, our result show that $\theta_{sm\text{-}t}$ transition shown as almost

302   flat wave-form; $\theta_{sm\text{-}t}$ did not change drastically during the first 75 % of SIs during the stance

303   phase, and the co-contraction associated with by part of the *m. quadriceps femoris* and the *m.*

304   *semimembranosus* seems to effectively supports the constant posture of the knee joint in most

305   terrestrial mammals. More than 80 % of the target animals in our study had similar θ_{ave} (100 ± 10

306   °) including species across a wide range of taxa, body masses, and locomotor modes, $\theta_{sm\text{-}t}$ is

307   measured from three points on the skeletons. Our findings indicate that θ_{ave} can be a useful

308   criteria for reconstructing the joint angles and posture of extinct mammals even if they have no

309   closely related extant descendants.

310

311   The correlation between body mass and θ_{ave} by taxon, and the angles unique to taxon and

312   locomotor modes suggest the possibility of applying a correction to 100 ± 10 ° that could be

313   applied to the all mammals. However, because our study focused on examining trends across a

314   wide range of taxa, the sample size for each taxon was small. Further data collection and

315   validation are required to obtain more accurate values for such corrections. In particular, our

316   results showed a significant difference between unguligrade and plantigrade, therefore, it would

317   apply more accurate correction if increase data. In addition, we found that *Suricata* had two

318   unique features: six out of the 13 $\theta_{sm\text{-}t}$ values were outliers when compared with the other species

319   (Fig. 4), and the difference between θ_{ave} and *Dolichotis*, which was the second smallest species

320   in this study, was more than 10 ° (Table 2 and Fig. 5). Furthermore, the difference between

321   *Suricata* and the next smallest species of Carnivora, *Felis*, was seven-fold in terms of body mass

322   and 20 ° in terms of θ_{ave}. However, the difference between *Felis* and the largest species of

323   Carnivora, *Ursus*, was greater than 20-fold in terms of body mass but less than 20 ° in terms of

324   θ_{ave} (Tables 1 and 2, Fig. 5). Therefore, it is possible that the *Suricata* data affected the *r* and

325   resulting *p*-value for Carnivora. This is probably because *Suricata* spends a lot of time

326   underground, which limits the required height to lift the trunk and limbs of the body. As such,

327   further data from subterranean species are necessary to confirm this hypothesis.

328

329   **Acknowledgements**

330   We thank Higashi Park Zoological Gardens, Higashiyama Zoo and Botanical Garden, Hitachi

331   Kaminé Zoo, Toyohashi Zoo and Botanical Park, and Ueno Zoological Garden for permission to

332   record the animals under their care. We also thank Yoko Tajima and Shin-ichiro Kawada

333   (National Museum of Nature and Science) for providing access to the extant mammal collections

334   under their care, and Naomi Wada (Yamaguchi University) for supplying the camera equipment.

335   We thank Katsuo Sashida (University of Tsukuba, now Mahidol University, Thailand), Sachiko

336 Agematsu (University of Tsukuba), Kohei Tanaka (University of Tsukuba, now Geological
337 Survey of Japan), Ikuko Tanaka (University of Tsukuba) and Yasunari Shigeta
338 (NMNS/University of Tsukuba) for providing helpful advice, discussion, and generous
339 encouragement during the course of our study. We would like to thank Editage
340 (www.editage.com) for English language editing. Finally, we greatly appreciate for editor and
341 reviewers to their helpful suggestions to improve this paper.
342

343 **References**

344 Alexander RM. 1991. Energy-saving mechanisms in walking and running. *The Journal of*
345   *Experimental Biology* 160:55–69.
346 Alexander RMN, Jayes AS. 1978. Vertical movements in walking and running. *Journal of*
347   *Zoology* 185:27–40. DOI: 10.1111/j.1469-7998.1978.tb03311.x.
348 Araújo JF, Rodrigues FB, Abadia FG, Gervásio FM, Mendonça GBN, Damasceno AD, Vieira
349   MF. 2016. Electromyographic analysis of the gait cycle phases of boxer dogs? *Brazilian*
350   *Journal of Veterinary and Animal Science* 68:931–937. DOI: 10.1590/1678-4162-8770.
351 Biewener AA. 1983. Allometry of quadrupedal locomotion: the scaling of duty factor, bone
352   curvature and limb orientation to body size. *The Journal of Experimental Biology* 105:147–
353   71.
354 Biewener AA. 1989. Scaling body support in mammals: limb posture and muscle mechanics.
355   *Science* 245:45–48. DOI: 10.1126/science.2740914.
356 Biewener AA. 1990. Biomechanics of mammalian terrestrial locomotion. *Science* 250:1097–
357   1103. DOI: 10.1126/science.2251499.
358 Biewener AA. 2005. Biomechanical consequences of scaling. *The Journal of Experimental*
359   *Biology* 208:1665–1676. DOI: 10.1242/jeb.01520.
360 Böhmer, C., Theil, J. C., Fabre, A. C., & Herrel, A. 2020. *Atlas of terrestrial mammal limbs*.
361   CRC Press.
362 Campos CM, Tognelli MF, Ojeda RA. 2001. Dolichotis patagonum. *Mammalian Species* 652:1–
363   5. DOI: 10.1644/1545-1410(2001)652<0001:DP>2.0.CO;2.
364 Cassinello J. 1997. High levels of inbreeding in captive Ammotragus lervia (Bovidae,
365   Artiodactyla): Effects on phenotypic variables. *Canadian Journal of Zoology* 75:1707–
366   1713. DOI: 10.1139/z97-797.
367 Cavagna GA, Heglund NC, Taylor CR. 1977. Mechanical work in terrestrial locomotion: two
368   basic mechanisms for minimizing energy expenditure. *American Journal of Physiology-*
369   *Regulatory, Integrative and Comparative Physiology* 233:R243–R261. DOI:
370   10.1152/ajpregu.1977.233.5.R243.
371 Day LM, Jayne BC. 2007. Interspecific scaling of the morphology and posture of the limbs

372   during the locomotion of cats (Felidae). *The Journal of Experimental Biology* 210:642–654.
373   DOI: 10.1242/jeb.02703.

374   Deban SM, Schilling N, Carrier DR. 2012. Activity of extrinsic limb muscles in dogs at walk,
375   trot and gallop. *The Journal of Experimental Biology* 215:287–300. DOI:
376   10.1242/jeb.063230.

377   Demes B, Larson SG, Stern JT, Jungers WL, Biknevicius AR, Schmitt D. 1994. The kinetics of
378   primate quadrupedalism: "hindlimb drive" reconsidered. *Journal of Human Evolution*
379   26:353–374. DOI: 10.1006/jhev.1994.1023.

380   Dick TJM, Clemente CJ. 2017. Where Have All the Giants Gone? How animals deal with the
381   problem of size. *PLOS Biology* 15:e2000473. DOI: 10.1371/journal.pbio.2000473.

382   Domning DP. 2002. The Terrestrial Posture of Desmostylians. *Smithsonian Contributions to*
383   *Paleobiology*.

384   Dutto DJ, Hoyt DF, Clayton HM, Cogger EA, Wickler SJ. 2006. Joint work and power for both
385   the forelimb and hindlimb during trotting in the horse. *The Journal of Experimental Biology*
386   209:3990–3999. DOI: 10.1242/jeb.02471.

387   Engberg I, Lundberg A. 1969. An electromyographic analysis of muscular activity in the
388   hindlimb of the cat during unrestrained locomotion. *Acta Physiologica Scandinavica*
389   75:614–630. DOI: 10.1111/j.1748-1716.1969.tb04415.x.

390   Fa JE, Purvis A. 1997. Body Size, Diet and Population Density in Afrotropical Forest Mammals:
391   A Comparison with Neotropical Species. *The Journal of Animal Ecology* 66:98. DOI:
392   10.2307/5968.

393   Fitzgerald CS, Krausman PR. 2002. Helarctos malayanus. *Mammalian Species* 696:1–5. DOI:
394   10.1644/1545-1410(2002)696<0001:HM>2.0.CO;2.

395   Fujiwara S. 2009. Olecranon orientation as an indicator of elbow joint angle in the stance phase,
396   and estimation of forelimb posture in extinct quadruped animals. *Journal of Morphology*
397   270:1107–1121. DOI: 10.1002/jmor.10748.

398   Fujiwara S, Hutchinson JR. 2012. Elbow joint adductor moment arm as an indicator of forelimb
399   posture in extinct quadrupedal tetrapods. *Proceedings of the Royal Society B: Biological*
400   *Sciences* 279:2561–2570. DOI: 10.1098/rspb.2012.0190.

401   Gambaryan PP. 1974. *How mammals run. Anatomical Adaptations*. New York. Halsted Press.

402   Garland T. 1983. The relation between maximal running speed and body mass in terrestruial
403   mammals. *Journal of Zoology* 199:157–170.

404   Gingerich PD. 2001. Origin of whales from early artiodactyls : hands and feet of Eocene
405   Protocetidae from Pakistan. *Science* 293:2239–2242. DOI: 10.1126/science.1063902.

406   Gingerich PD, Heissig K, Bebej RM, von Koenigswald W. 2017. Astragali of Pakicetidae and
407   other early-to-middle Eocene archaeocetes (Mammalia, Cetacea) of Pakistan: locomotion

408 and habitat in the initial stages of whale evolution. *PalZ* 91:601–627. DOI: 10.1007/s12542-
409 017-0362-8.

410 Gingerich PD, Ul-Haq M, Von Koenigswald W, Sanders WJ, Smith BH, Zalmout IS. 2009. New
411 protocetid whale from the middle Eocene of Pakistan: Birth on land, precocial development,
412 and sexual dimorphism. *PLoS ONE* 4. DOI: 10.1371/journal.pone.0004366.

413 Griffin TM, Main RP, Farley CT. 2004. Biomechanics of quadrupedal walking: How do four-
414 legged animals achieve inverted pendulum-like movements? *Journal of Experimental*
415 *Biology* 207:3545–3558. DOI: 10.1242/jeb.01177.

416 Haas SK, Hayssen V, Krausman PR. 2005. Panthera leo. *Mammalian Species* 762:1–11.

417 Hildebrand M. 1984. Rotations of the Leg Segments of Three Fast-Running Cursors and an
418 Elephant. *Journal of Mammalogy* 65:718–720. DOI: 10.2307/1380866.

419 Hildebrand M, Hurley JP. 1985. Energy of the oscillating legs of a fast-moving cheetah,
420 pronghorn, jackrabbit, and elephant. *Journal of Morphology* 184:23–31. DOI:
421 10.1002/jmor.1051840103.

422 Hillman-Smith AKK, Groves CP. 1994. Diceros bicornis. *Mammalian Species* 455:1. DOI:
423 10.2307/3504292.

424 Hogan N. 1984. Adaptive Control of Mechanical Impedance by Coactivation of Antagonist
425 Muscles. *IEEE Transactions on Automatic Control* 29:681–690. DOI:
426 10.1109/TAC.1984.1103644.

427 Inuzuka N. 1988. Reconstruction of Extinct Mammal, Desmostylus (In Japanese).
428 *Biomechanisms* 9:7–19. DOI: 10.3951/biomechanisms.9.7.

429 Inuzuka N. 1996. Preriminary study on kinematic gait analysis in mammals. *Mammal Study*
430 21:43–57.

431 Inuzuka N, Sawamura H, Watabe H. 2006. Paleoparadoxia and the Nishikurosawa specimen
432 from Oga (In Japanese), *Akita, northern Japan*. Akita, Japan.

433 Knarr BA, Zeni JA, Higginson JS. 2012. Comparison of electromyography and joint moment as
434 indicators of co-contraction. *Journal of Electromyography and Kinesiology* 22:607–611.
435 DOI: 10.1016/j.jelekin.2012.02.001.

436 Louie JK, Mote CD. 1987. Contribution of the musculature to rotatory laxity and torsional
437 stiffness at the knee. *Journal of Biomechanics* 20:281–300. DOI: 10.1016/0021-
438 9290(87)90295-8.

439 Madar SI. 2007. The postcranial skeleton of early Eocene pakicetid cetaceans. *Journal of*
440 *Paleontology* 81:176–200. DOI: 10.1666/0022-3360(2007)81[176:TPSOEE]2.0.CO;2.

441 Mech LD. 1974. Canis Lupus. *Mammalian Species* 37:1–6. DOI: 10.2307/3503924.

442 Nielsen J, Sinkjær T, Toft E, Kagamihara Y. 1994. Segmental reflexes and ankle joint stiffness
443 during co-contraction of antagonistic ankle muscles in man. *Experimental Brain Research*

444   102:350–358. DOI: 10.1007/BF00227521.

445 O'Connor SM, Dawson TJ, Kram R, Donelan JM. 2014. The kangaroo ' s tail propels and

446   powers pentapedal locomotion. *Biology Letters* 10:1–5. DOI: 10.1098/rsbl.2014.0381.

447 Obara H, Uramoto M, Hidetoshi O, Matsui M. 2000. Japanese macaque. In *Animal world*

448   *helitage Red data animals* (Japanese). Tokyo: Kodansha Ltd, 139.

449 Olmstead TG, Wevers HW, Bryant JT, Gouw GJ. 1986. Effect of muscular activity on

450   valgus/varus laxity and stiffness of the knee. *Journal of Biomechanics* 19:565–577. DOI:

451   10.1016/0021-9290(86)90162-4.

452 Padilla M, Dowler RC. 1994. Tapirus terrestris. *Mammalian Species* 481:1–8. DOI:

453   10.1007/978-1-4615-6434-8_37.

454 Patel BA, Horner AM, Thompson NE, Barrett L, Henzi SP. 2013. Ontogenetic scaling of fore-

455   and hind limb posture in wild chacma baboons (Papio hamadryas ursinus). *PLoS ONE* 8:1–

456   8. DOI: 10.1371/journal.pone.0071020.

457 Polly PD. 2007. Limbs in mammalian evolution. In: Hall BK ed. *Fins into Limbs: Ecolution,*

458   *Development, and Transformation*. Chicago: University of Chicago Press, 245–268.

459 Ren L, Butler M, Miller C, Paxton H, Schwerda D, Fischer MS, Hutchinson JR. 2008. The

460   movements of limb segments and joints during locomotion in African and Asian elephants.

461   *The Journal of Experimental Biology* 211:2735–2751. DOI: 10.1242/jeb.018820.

462 Riemann BL, Lephart SM. 2002. The sensorimotor system, Part II: The role of proprioception in

463   motor control and functional joint stability. *Journal of Athletic Training* 37:80–84. DOI:

464   10.1016/j.jconhyd.2010.08.009.

465 Shikama T. 1966. Postcranial Skeltons of Japanese Desmostylia. *Paleontological Society of*

466   *Japan Special Papers* 12:1–241.

467 Shoshani J, Eisenberg JF. 1982. Elephas maximus. *Mammalian Species* 182:1–8.

468 Thewissen JGM, Illiams EM, Roe LJ, Hussain ST. 2001. Skeletons of terrestrial cetacean and the

469   relationship of whales to ariodactyls. *Nature* 413:277–281.

470 Thewissen JGM, Madar SI, Hussain ST. 1998. Whale ankles and evolutionary relationships.

471   *Nature* 395:452. DOI: 10.1038/26656.

472 Tokuriki M. 1973. Electoromyographic and Joint-Mechanical Studies in Quadrupedal

473   Locomotion: I. WALK. *The Japanese Journal of Veterinary Science* 35:433-446_2. DOI:

474   10.1292/jvms1939.35.433.

475 van Staaden MJ. 1994. Suricata suricatta. *Mammalian Species* 483:1. DOI: 10.2307/3504085.

476

Figure 1

A model of the mammalian hindlimb bones with *m. semimembranosus* from the exterior view.

M. semimembranosus origin locates on the ischial tuberosity (IT) and insertion locates on the interior-proximal end of the tibia (T). The insertion of this muscle was drawn on the exterior of tibia in this figure to identify the position easily, however, the actual insertion locates on the interior of tibia. Abbreviations: (F) femur, (IT) ischial tuberosity, (MS) *m. semimembranosus*, (P) pelvis, and (T) tibia.
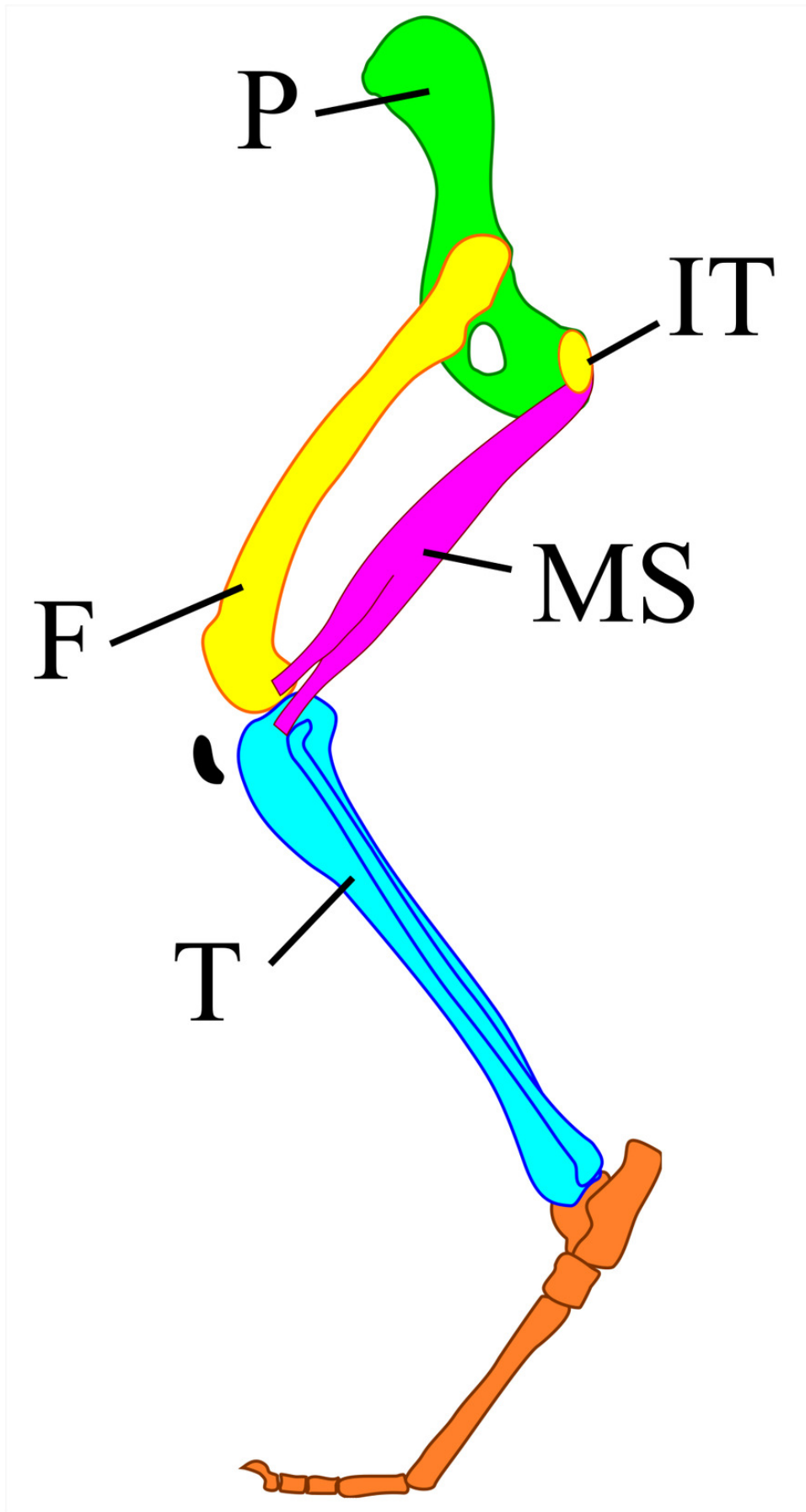
Figure 2

(A) How the measured pictures were picked. (B) The line of measured angle on walking cat.

(A) A period between touched down to the next touched down was converted to still images. The pictures covered in blue were the first 75 % of the total still images. Calculated from the number of first 75% to obtain 13 pictures to measure from the first and the last combined at 12 equal intervals.

The numbers in each box are measured pictures. The calculation for intervals is: (number of first 75 % of still images) / (13-1) = Interval

(B) A pink line represents a line of action of m. semimembranosus. A blue line represents line of axis of tibia. A yellow area is an angle where is measured.
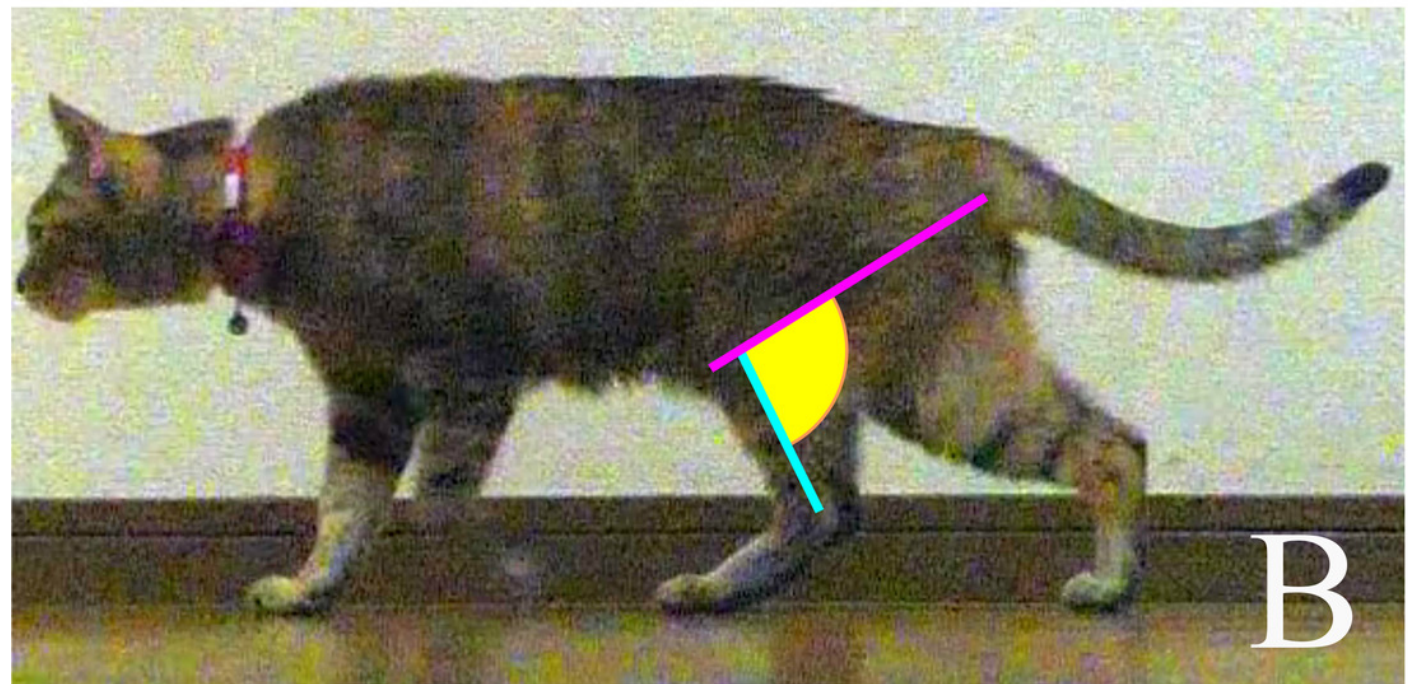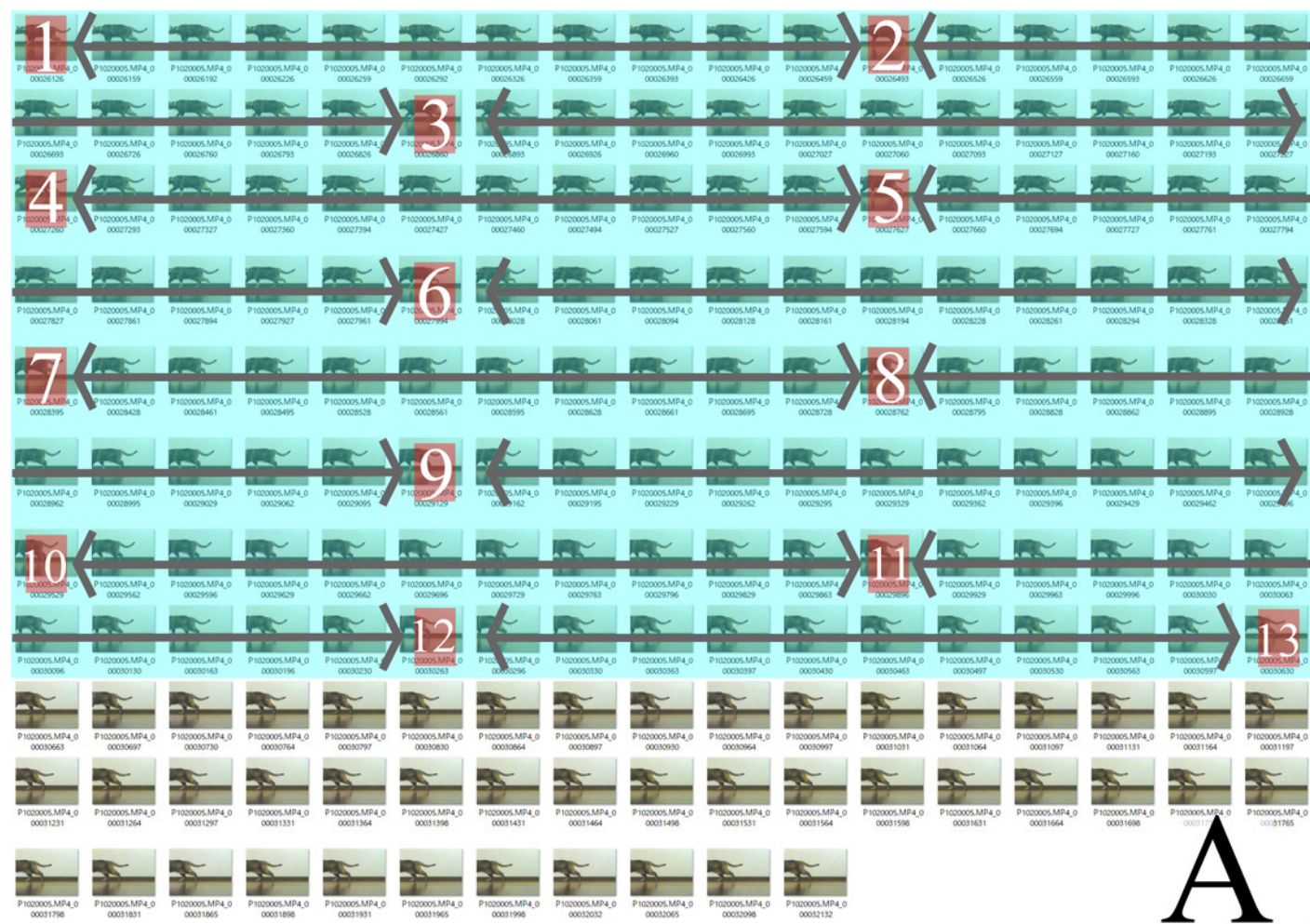
Figure 3

The box plots of θ_{sm-t} of stances of each target animals.

The x-axis shows the name of species and y-axis shows the angles in degrees. The thick bar in each box shows the median value. The top of each box shows the third quartile point, the bottom shows the first quartile point.
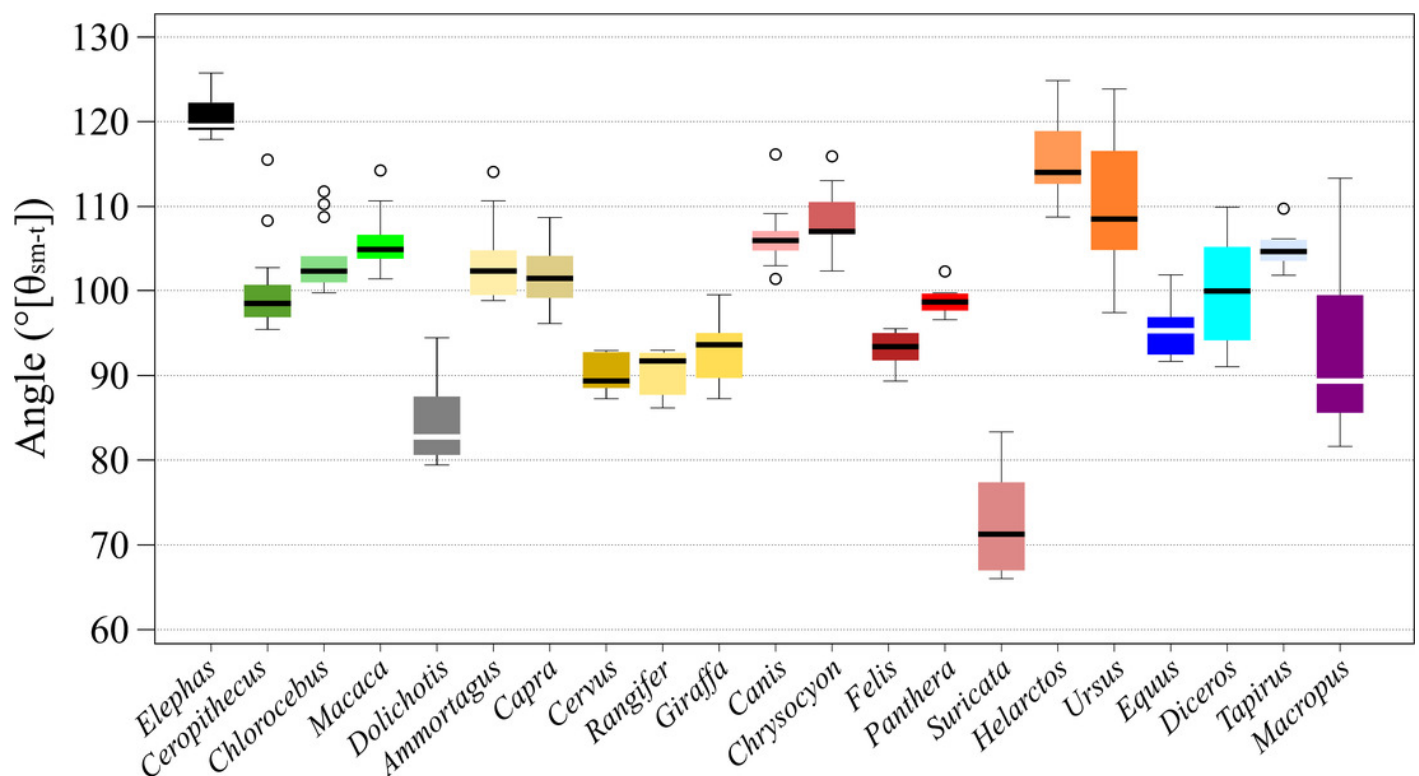
Figure 4

The line and box charts of $\theta_{sm\text{-}t}$ transition of stances of each target animals.

The x-axis shows SIs and the y-axis shows the $\theta_{sm\text{-}t}$ in degrees. Each line and plot color are identical to the colors of each box in Fig. 2. The circle plots showed the plantigrades, the triangle plots show the unguligrade, the square plots show the digitigrades, and an asterisk show other walk style. The top and bottom bars showed the maximum angles and the smallest angles, respectively. The plots under bars are outliers.
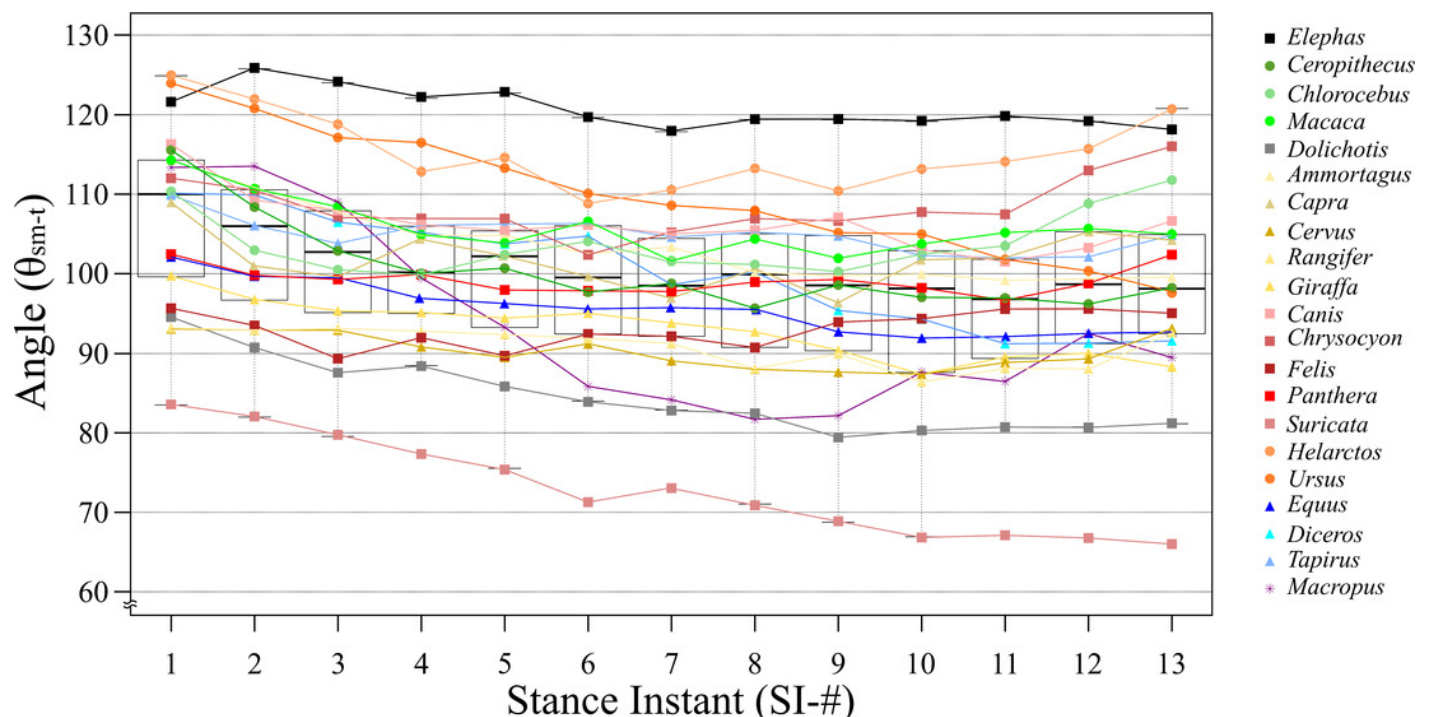
Figure 5

A scatter chart of the body mass and θ_{ave}.

The x-axis shows the body mass in the log of kg and the y-axis shows the θ_{ave}. Each plot color is identical to the colors of each box in Fig. 2. The circle plots showed the plantigrades, the triangle plots show the unguligrade, the square plots show the digitigrades, and an asterisk shows another walk style.
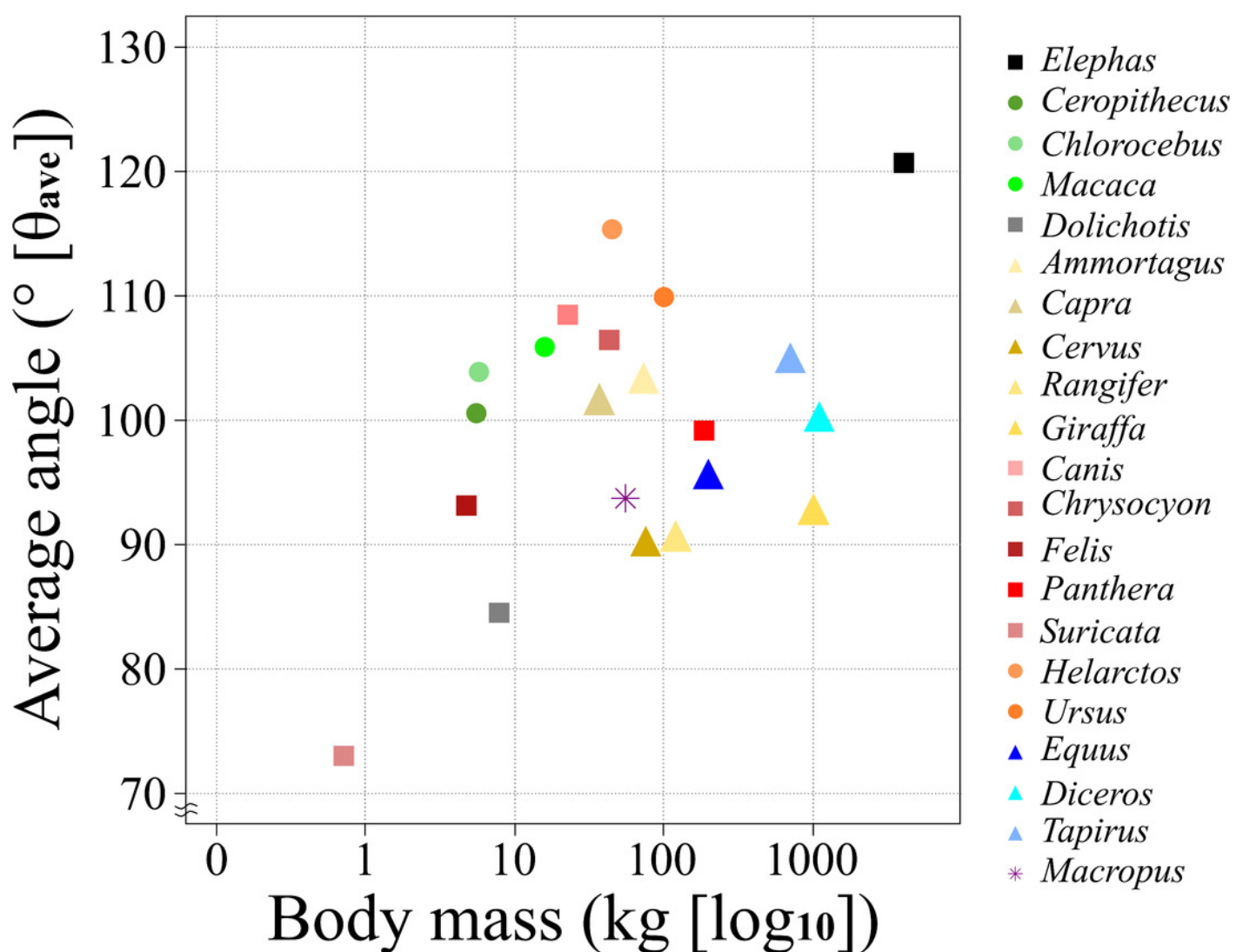
Figure 6

A box plot of θ_{ave} of each ambulatory style.

The x-axis shows the locomotor modes and the y-axis shows the θ_{ave}. Each plot color is identical to the colors of each box in Fig. 2. The circle plots showed the plantigrades, the triangle plots show the unguligrade, the square plots show the digitigrades.
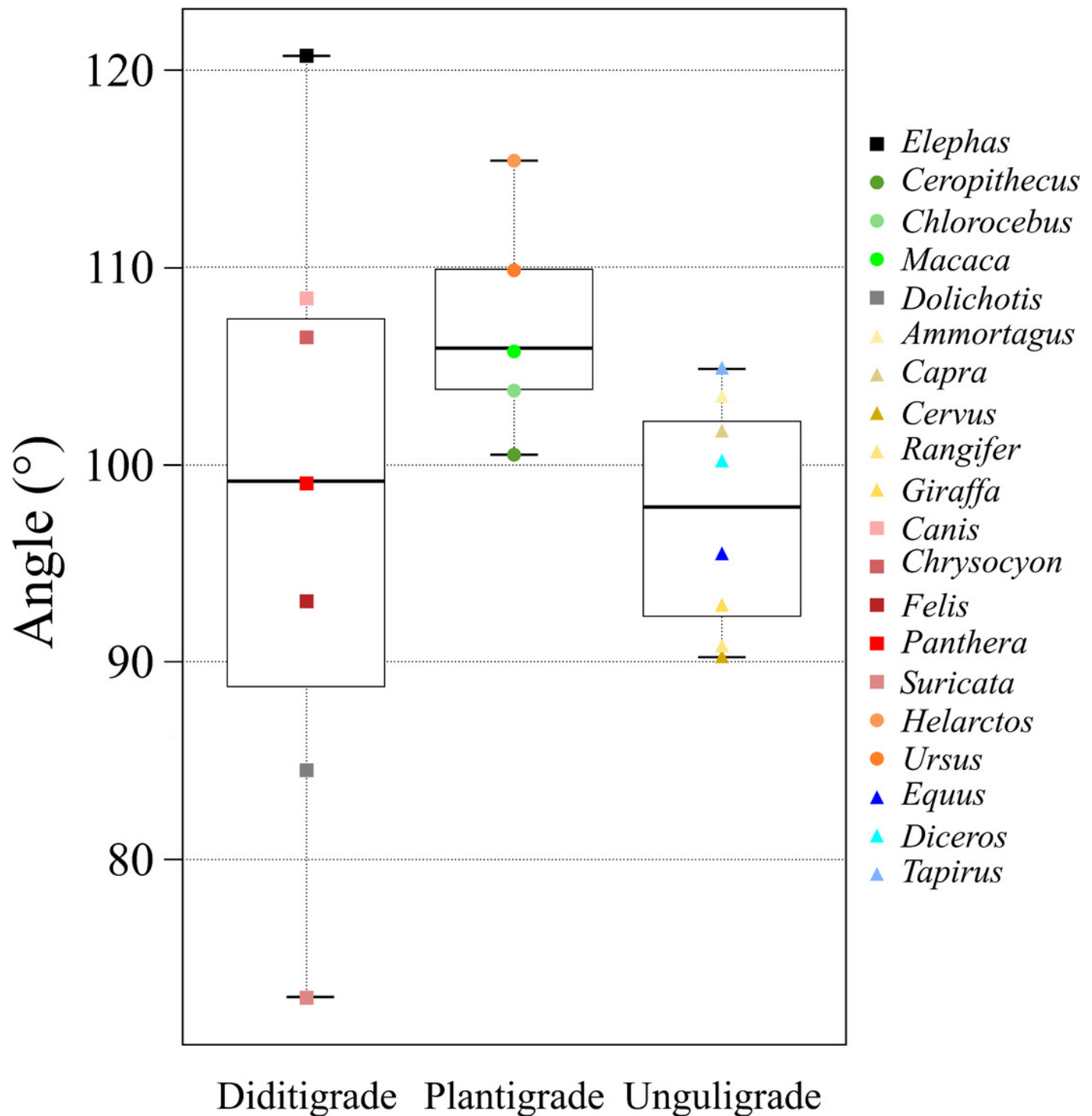
A list of the target animals of this study.

The body mass data are the average of the data from reference or each zoo. Ambulatory style abbreviations: (U) unguligrade, (D) digitigrade, (P) plantigrade, and (O) other. Institutional abbreviations: (HKZ) Hitachi Kamine Zoo, Ibaraki; (HP) Higashi Park Zoological Gardens, Aichi; (HZ) Higashiyama Zoo and Botanical Garden, Aichi; (TZ) Toyohashi Zoo and Botanical Park, Aichi; and (UZ) Ueno Zoo, Tokyo. Institutions are sorted by alphabetical order.

Super Order	Order	Family	Genus	Species	Locomotor mode	Locality	Body Mass (kg)	Body Mass Reference
Afrotheria	Proboscidea	Elephantidae	*Elephas*	*maximus*	D	UZ	4060.0	Shoshani & Eisenberg (1982)
Euarchonto-glires	Primates	Ceropithecidae	*Cercopithecus*	*neglectus*	P	UZ	4.5	Fa & Purvis (1997)
			Chlorocebus	*aethiops*	P	HKZ	5.78	Our study
			Macaca	*fuscata*	P	HKZ	16.0	Obara et al. (2000)
	Rodentia	Cavidae	*Dolichotis*	*patagonum*	D	HP	8.0	Campos et al. (2001)
Laurasia-theria	Artiodactyla	Bovidae	*Ammotragus*	*lervia*	U	UZ	72.6	Cassinello (1997)
			Capra	*hircus*	U	HKZ	37.0	Our study
		Cervidae	*Cervus*	*nippon*	U	UZ	75.4	Our study
			Rangifer	*tarandus*	U	HZ	120.0	Garland (1983)
		Giraffidae	*Giraffa*	*camelopardalis*	U	UZ	1000.0	Garland (1983)
	Carnivora	Canidae	*Canis*	*lupus*	D	HZ	43.3	Mech (1974)
			Chrysocyon	*brachyurus*	D	UZ	23.0	Our study
		Felidae	*Felis*	*catus*	D	Co	4.8	Our study
			Panthera	*leo*	D	TZ	188.0	Haas et al. (2005)
		Herpestidae	*Suricata*	*suricatta*	D	HP	0.7	van Staaden (1994)
		Ursidae	*Helarctos*	*malayanus*	P	TZ	45.0	Fitzgerald & Krausman (2002)
			Ursus	*thibetanus*	P	HKZ	100.0	Our study
	Perissodactyla	Equidae	*Equus*	*cabullus*	U	TZ	200.0	Garland (1983)
		Rhinocerotidae	*Diceros*	*bicornis*	U	UZ	1100.0	Hillman-Smith & Groves (1994)
		Tapiridae	*Tapirus*	*terrestris*	U	HZ	700.0	Padilla & Dowler (1994)
Marspialia	Diprotodontia	Macropodidae	*Macropus*	*giganteus*	O	UZ	55.0	Our study

Angles between the tibia shaft and *m. semimembranosus* in taxonomical order*.*

The angle data are the average of three stances collected in our study. The differences between the maximum and the minimum angle were calculated (Diff). To visualize the variability, the standard deviation of each row and column was also calculated (SD). The raw data are in the appendix.

Target	SI-1	SI-2	SI-3	SI-4	SI-5	SI-6	SI-7	SI-8	SI-9	SI-10	SI-11	SI-12	SI-13	Diff.	θ_{ave}	SD
Proboscidea																
Elephas	121.6	125.8	124.1	122.1	122.8	119.7	117.9	119.5	119.5	119.2	119.8	119.2	118.1	7.9	120.7	2.40
Primates																
Cercopithecus	115.6	108.4	102.8	100.2	100.7	97.7	98.8	95.6	95.5	97.0	96.9	96.3	98.2	20.1	100.3	5.64
Chlorocebus	110.3	102.9	100.6	100.0	102.4	104.1	101.7	101.1	100.4	102.5	103.5	108.8	111.9	11.9	103.9	3.94
Macaca	114.3	110.8	108.3	104.9	103.9	106.7	101.5	104.3	102.0	103.8	105.2	105.7	104.9	12.8	105.9	3.52
Diff.	5.3	7.9	7.7	4.9	3.2	9.0	2.9	8.7	6.5	6.8	8.3	12.5	13.7			
SD	2.75	4.06	3.99	2.78	1.61	4.63	1.61	4.43	1.75	3.58	4.42	6.51	6.87			
Rodentia																
Dolichotis	94.5	90.8	87.6	88.4	85.9	83.9	82.9	82.5	79.5	80.3	80.7	80.7	81.2	15.0	84.5	4.61
Artiodactyla																
Ammotragus	114.2	110.7	107.8	104.7	104.8	102.4	103.4	100.1	99.6	99.8	99.0	99.1	99.5	15.2	103.5	4.87
Capra	108.8	101.0	99.5	104.4	102.2	99.5	97.0	100.5	96.3	101.7	102.0	105.3	104.1	12.5	101.7	3.41
Cervus	93.1	92.8	92.9	90.7	89.5	91.1	89.0	87.9	87.5	87.3	88.9	89.3	93.1	5.8	90.2	2.18
Rangifer	93.0	92.8	93.0	92.7	92.2	91.7	91.2	87.9	89.8	86.3	87.9	88.1	92.5	6.7	90.7	2.39
Giraffa	99.7	96.7	95.1	94.9	94.6	94.9	93.8	92.6	90.3	87.3	89.4	89.8	88.1	12.4	92.9	3.65
Diff.	21.2	17.9	14.9	14.0	15.3	11.3	14.4	12.6	12.1	15.4	14.1	17.2	16.0			
SD	9.47	7.44	6.26	6.63	6.59	4.92	5.61	6.23	5.02	7.57	6.54	7.55	6.32			
Carnivora																
Canis	116.2	109.2	108.0	106.2	105.4	106.1	105.0	105.5	107.2	103.0	101.7	103.3	106.7	14.5	95.6	3.59
Chrysocyon	112.0	110.5	107.1	106.9	106.9	102.5	105.1	106.9	106.7	107.8	107.6	113.1	116.1	13.6	108.4	3.62
Felis	95.6	93.6	89.5	91.9	89.6	92.4	92.2	90.8	93.9	94.4	95.7	95.6	95.0	6.2	93.1	2.20
Panthera	102.4	99.6	99.1	99.9	97.9	97.7	97.8	98.8	99.2	98.2	96.6	98.8	102.5	5.9	99.1	1.73
Suricata	83.5	82.0	79.6	77.3	75.5	71.3	73.1	71.0	68.8	66.9	67.1	66.7	66.0	17.5	73.0	6.09

Helarctos	125.0	122.1	118.8	112.9	114.6	108.8	110.6	113.3	110.4	113.2	114.2	115.5	120.8	16.2	115.4	4.89
Ursus	124.0	120.8	117.1	116.5	113.3	110.1	108.6	108.1	105.1	104.9	101.9	100.4	97.5	26.5	109.9	8.08
Diff.	41.5	40.1	39.2	39.2	39.1	18.8	37.5	42.3	41.6	46.3	47.1	48.8	54.8			
SD	15.32	14.59	14.34	13.46	14.02	13.48	13.02	14.38	14.32	15.18	14.97	16.08	17.93			
Perissodactyla																
Equus	102.8	99.7	99.5	96.8	96.2	95.3	95.6	95.3	92.5	91.7	92.0	92.4	92.5	11.1	95.6	3.32
Diceros	110.0	109.9	106.5	105.3	103.7	104.8	98.6	100.0	95.4	94.3	91.1	91.1	91.5	18.9	100.2	7.01
Tapirus	109.9	106.0	103.6	106.0	106.3	106.3	104.5	105.1	104.9	102.2	102.0	102.0	104.8	7.9	104.9	2.19
Diff.	7.2	10.2	7.0	9.2	10.1	11.0	8.9	9.8	12.4	10.5	10.9	10.9	13.3			
SD	4.55	5.13	3.51	5.09	5.22	5.96	4.51	4.90	6.45	5.43	6.03	5.92	7.38			
Diprotodontia																
Macropus	113.4	113.6	109.0	99.4	93.2	85.7	84.1	81.8	82.1	87.6	86.4	92.5	89.4	31.8	93.7	11.50
Total																
Diff.	41.5	43.8	44.5	44.8	47.3	48.4	44.8	48.5	50.7	52.3	52.7	52.5	54.8			
Mean	107.6	104.7	102.4	101.1	100.1	98.7	97.7	97.6	96.5	96.6	96.6	97.8	98.8		99.7	
SD	11.18	11.18	10.73	10.03	10.64	10.61	10.22	11.33	11.39	11.66	11.56	12.05	12.81			

Angles between the tibia shaft and *m. semimembranosus* in ambulator style order.

Data for each SI angle are the same as in Table 2. The θ_{ave} are the average values of each stance (a series of SI-1 to SI-13). The differences between the maximum and the minimum angle were calculated (Diff). To visualize the variability, the standard deviation of each row and column was also calculated (SD). The raw data are in the appendix.

Ambulatory style	SI-1	SI-2	SI-3	SI-4	SI-5	SI-6	SI-7	SI-8	SI-9	SI-10	SI-11	SI-12	SI-13	θ_{ave}	SD
Unguligrade															
Ammotragus	114.2	110.7	107.8	104.7	104.8	102.4	103.4	100.1	99.6	99.8	99.0	99.1	99.5	103.5	4.87
Capra	108.8	101.0	99.5	104.4	102.2	99.5	97.0	100.5	96.3	101.7	102.0	105.3	104.1	101.7	3.41
Cervus	93.1	92.8	92.9	90.7	89.5	91.1	89.0	87.9	87.5	87.3	88.9	89.3	93.1	90.2	2.18
Rangifer	93.0	92.8	93.0	92.7	92.2	91.7	91.2	87.9	89.8	86.3	87.9	88.1	92.5	90.7	2.39
Giraffa	99.7	96.7	95.1	94.9	94.6	94.9	93.8	92.6	90.3	87.3	89.4	89.8	88.1	92.9	3.65
Equus	102.8	99.7	99.5	96.8	96.2	95.3	95.6	95.3	92.5	91.7	92.0	92.4	92.5	95.6	3.32
Diceros	110.0	109.9	106.5	105.3	103.7	104.8	98.6	100.0	95.4	94.3	91.1	91.1	91.5	100.2	7.01
Tapirus	109.9	106.0	103.6	106.0	106.3	106.3	104.5	105.1	104.9	102.2	102.0	102.0	104.8	104.9	2.19
Diff.	21.25	17.9	14.9	15.3	16.8	15.2	15.5	17.2	17.4	15.9	14.1	17.2	16.7		
SD	8.10	7.08	5.84	6.31	6.37	5.85	5.45	6.31	5.72	6.68	5.96	6.55	6.22		
Digitigrade															
Elephas	121.6	125.8	124.1	122.1	122.8	119.7	117.9	119.5	119.5	119.2	119.8	119.2	118.1	120.7	2.40
Dolichotis	94.5	90.8	87.6	88.4	85.9	83.9	82.9	82.5	79.5	80.3	80.7	80.7	81.2	84.5	4.61
Canis	116.2	109.2	108.0	106.2	105.4	106.1	105.0	105.5	107.2	103.0	101.7	103.3	106.7	95.6	3.59
Chrysocyon	112.0	110.5	107.1	106.9	106.9	102.5	105.1	106.9	106.7	107.8	107.6	113.1	116.1	108.4	3.62
Felis	95.6	93.6	89.5	91.9	89.6	92.4	92.2	90.8	93.9	94.4	95.7	95.6	95.0	93.1	2.20
Panthera	102.4	99.6	99.1	99.9	97.9	97.7	97.8	98.8	99.2	98.2	96.6	98.8	102.5	99.1	1.73
Suricata	83.5	82.0	79.6	77.3	75.5	71.3	73.1	71.0	68.8	66.9	67.1	66.7	66.0	73.0	6.09
Diff.	38.1	43.3	44.5	44.8	47.3	48.4	44.8	48.5	50.7	52.3	52.7	52.5	52.1		
SD	13.56	14.69	15.12	14.63	15.67	15.68	15.04	16.33	17.39	17.44	17.33	18.18	18.92		
Plantigrade															
Cercopithecus	115.6	108.4	102.8	100.2	100.7	97.7	98.8	95.6	95.5	97.0	96.9	96.3	98.2	100.3	5.64
Chlorocebus	110.3	102.9	100.6	100.0	102.4	104.1	101.7	101.1	100.4	102.5	103.5	108.8	111.9	103.9	3.94

Macaca	114.3	110.8	108.3	104.9	103.9	106.7	101.5	104.3	102.0	103.8	105.2	105.7	104.9	105.9	3.52
Helarctos	125.0	122.1	118.8	112.9	114.6	108.8	110.6	113.3	110.4	113.2	114.2	115.5	120.8	115.4	4.89
Ursus	124.0	120.8	117.1	116.5	113.3	110.1	108.6	108.1	105.1	104.9	101.9	100.4	97.5	109.9	8.08
Diff.	14.7	19.2	18.2	16.5	13.9	12.4	11.8	17.7	14.9	16.2	17.3	19.2	23.3		
SD	8.10	7.08	5.84	6.31	6.37	5.85	5.45	6.31	5.72	6.68	5.96	6.55	6.22		
Other															
Macropus	113.4	113.6	109.0	99.4	93.2	85.7	84.1	81.8	82.1	87.6	86.4	92.5	89.4	93.7	11.50

Subtracted values of each SIs: subtracted $\theta_{sm\text{-}t}$ less the previous $\theta_{sm\text{-}t}$.

Each cell shows the subtracted value of $\theta_{sm\text{-}t}$. The italics cells show negative values.

Locomotor mode abbreviations are the same as in Table 1.

Target	SI1-SI2	SI2-SI3	SI3-SI4	SI4-SI5	SI5-SI6	SI6-SI7	SI7-SI8	SI8-SI9	SI9-SI10	SI10-SI11	SI11-SI12	SI12-SI13	Amb Style
Elephas	*-4.25*	**1.71**	**1.97**	*-0.66*	**3.11**	**1.75**	*-1.52*	**0.00**	**0.29**	*-0.64*	0.62	**1.05**	D
Cercopithecus	**7.21**	**5.62**	**2.61**	*-0.52*	2.97	*-1.08*	**3.23**	*-2.97*	**1.50**	**0.19**	**0.53**	*-1.83*	P
Chlorocebus	**7.42**	**2.33**	**0.61**	*-2.46*	*-1.67*	**2.43**	**0.57**	**0.71**	*-2.14*	*-0.98*	*-5.32*	*-3.07*	P
Macaca	**3.49**	**2.51**	**3.44**	**0.97**	*-2.81*	**5.19**	*-2.82*	**2.30**	*-1.73*	*-1.46*	*-0.48*	**0.78**	P
Dolichotis	**3.73**	**3.20**	*-0.86*	**2.47**	**2.00**	**1.07**	**0.35**	**3.02**	*-0.81*	*-0.34*	*-0.05*	*-0.46*	D
Ammotragus	**3.48**	**2.88**	**3.07**	*-0.10*	**2.40**	*-0.94*	**3.30**	0.51	*-0.23*	**0.81**	*-0.19*	*-0.32*	U
Capra	**7.79**	**1.53**	*-4.93*	**2.26**	**2.66**	**2.51**	*-3.47*	**4.19**	*-5.39*	*-0.28*	*-3.33*	**1.20**	U
Cervus	**0.28**	*-0.06*	**2.19**	**1.15**	*-1.60*	**2.13**	**1.13**	**0.36**	**0.22**	*-1.57*	*-0.43*	*-3.76*	U
Rangifer	**0.19**	*-0.22*	**0.31**	**0.55**	**0.47**	**0.52**	**3.30**	*-1.95*	**3.51**	*-1.54*	*-0.19*	*-4.42*	U
Giraffa	**3.00**	**1.60**	**0.19**	**0.69**	*-0.67*	**1.14**	**1.17**	**2.30**	**2.98**	*-2.11*	*-0.37*	**1.76**	U
Canis	**6.97**	**1.29**	**1.71**	**0.80**	*-0.62*	**1.03**	*-0.46*	*-1.68*	**4.16**	**1.35**	*-1.64*	*-3.42*	D
Chrysocyon	**1.49**	**3.41**	**0.13**	*-0.02*	**4.49**	*-2.67*	*-1.8*	**0.24**	*-1.12*	**0.24**	*-5.56*	*-3.01*	D
Felis	**2.03**	**4.02**	*-2.36*	**2.32**	*-2.84*	**0.24**	**1.40**	*-3.08*	*-0.51*	*-1.29*	**0.08**	**0.55**	D
Panthera	**2.79**	**0.49**	*-0.75*	**2.02**	**0.16**	*-0.07*	*-1.00*	*-0.41*	**0.96**	**1.58**	*-2.12*	*-3.76*	D
Suricata	**1.56**	**2.41**	**2.25**	**1.85**	**4.18**	*-1.85*	**2.14**	**2.21**	**1.92**	*-0.22*	**0.44**	**0.66**	D
Helarctos	**2.91**	**3.30**	**5.90**	*-1.65*	**5.76**	*-1.80*	*-2.70*	**2.89**	*-2.87*	*-0.94*	*-1.33*	*-5.30*	P
Ursus	**3.19**	**3.66**	**0.58**	**3.24**	**3.22**	**1.46**	**0.56**	**2.92**	**0.23**	**3.02**	**1.50**	**2.87**	P
Equus	**2.36**	**0.18**	**2.73**	**0.63**	**0.88**	*-0.32*	**0.29**	**2.78**	**0.82**	*-0.31*	*-0.41*	*-0.07*	U
Diceros	**0.16**	**3.36**	**1.21**	**1.61**	*-1.15*	**6.27**	*-1.43*	**4.57**	**1.15**	**3.19**	*-0.05*	*-0.37*	U
Tapirus	**3.90**	**2.43**	*-2.37*	*-0.29*	**0.01**	**1.76**	*-0.64*	**0.27**	**2.71**	**0.17**	*-0.01*	*-2.79*	U
Macropus	*-0.20*	**4.55**	**9.63**	**6.17**	**7.47**	**1.63**	**2.27**	*-0.33*	*-5.38*	**1.14**	*-6.10*	**3.07**	O

A list of correlation coefficient (*r*) values and each *p*-value.

Body mass of X	Correlation coefficient	P-value (< 0.05)	Degrees of freedom
All	0.19	0.55	19
Primates	0.81	0.40	1
Artiodactyla	-0.46	0.44	3
Carnivora	0.81	0.028	5
Perissodactyla	0.71	0.49	1
Plantigrade	0.82	0.09	3
Digitigrade	0.88	0.01	5
Unguligrade	0.07	0.87	6

Results of (A) ANOVA and (B) multiple comparisons.

List (A) shows results of one-way ANOVA. List (B) shows results of multiple comparisons.

Abbreviations: degree of freedom (d.f.); difference (diff.).

1   A. One-way ANOVA

Explanatory variable	F-value	Numerator d.f.	Denominator d.f.	p-value
Taxa	1.62	3.00	6.82	0.27
Ambulatory style	4.16	2.00	9.80	0.049
Body mass	0.67	3.00	6.03	0.60

3   B. Multiple comparisons

Pair		Mean diff.	Standard error	d.f.	p-value
Unguligrade digitigrade	vs.	0.44	6.38	7.40	0.997
Unguligrade plantigrade	vs.	9.65	3.29	8.77	0.041
Digitigrade plantigrade	vs.	-9.21	6.55	7.97	0.383